

# Journal of Biomedical Optics

BiomedicalOptics.SPIEDigitalLibrary.org

## **Targeted imaging of cancer by fluorocoxib C, a near-infrared cyclooxygenase-2 probe**

Md. Jashim Uddin  
Brenda C. Crews  
Kebreab Ghebreselasie  
Cristina K. Daniel  
Philip J. Kingsley  
Shu Xu  
Lawrence J. Marnett

# Targeted imaging of cancer by fluorocoxib C, a near-infrared cyclooxygenase-2 probe

Md. Jashim Uddin,\* Brenda C. Crews, Kebreab Ghebreselasie, Cristina K. Daniel, Philip J. Kingsley, Shu Xu, and Lawrence J. Marnett  
Vanderbilt University School of Medicine, Vanderbilt-Ingram Cancer Center, Vanderbilt Institute of Chemical Biology, A. B. Hancock, Jr., Memorial Laboratory for Cancer Research, Department of Biochemistry, Chemistry and Pharmacology, Nashville, Tennessee 37232-0146, United States

**Abstract.** Cyclooxygenase-2 (COX-2) is a promising target for the imaging of cancer in a range of diagnostic and therapeutic settings. We report a near-infrared COX-2-targeted probe, fluorocoxib C (FC), for visualization of solid tumors by optical imaging. FC exhibits selective and potent COX-2 inhibition in both purified protein and human cancer cell lines. *In vivo* optical imaging shows selective accumulation of FC in COX-2-overexpressing human tumor xenografts [1483 head and neck squamous cell carcinoma (HNSCC)] implanted in nude mice, while minimal uptake is detectable in COX-2-negative tumor xenografts (HCT116) or 1483 HNSCC xenografts preblocked with the COX-2-selective inhibitor celecoxib. Time course imaging studies conducted from 3 h to 7-day post-FC injection revealed a marked reduction in nonspecific fluorescent signals with retention of fluorescence in 1483 HNSCC tumors. Thus, use of FC in a delayed imaging protocol offers an approach to improve imaging signal-to-noise that should improve cancer detection in multiple preclinical and clinical settings. © The Authors. Published by SPIE under a Creative Commons Attribution 3.0 Unported License. Distribution or reproduction of this work in whole or in part requires full attribution of the original publication, including its DOI. [DOI: 10.1117/1.JBO.20.5.050502]

Keywords: cyclooxygenase-2; fluorocoxib C; optical imaging; cancer; delayed imaging.

Paper 150126LR received Mar. 6, 2015; accepted for publication Apr. 15, 2015; published online May 13, 2015.

Fluorescent contrast agents that emit light in the near-infrared (NIR) region are particularly useful for *in vivo* imaging targeted to the early detection of cancer.<sup>1</sup> In the last decade, technological advances have led to the development of target-directed NIR probes for imaging or image-guided surgery.<sup>1,2</sup> However, their nonspecific biodistribution and inefficient clearance from nontargeted organs are obstacles to achieving high signal-to-noise ratios in the short-term following administration.<sup>3</sup> One way to address this problem would be through probes that not only absorb and emit at the NIR region, but are also selectively

retained at the target, thereby providing time for clearance from nontarget sites. In fact, some reports have demonstrated an advantage of delayed imaging (up to 3 h) of tumors using [<sup>18</sup>F]-fluorodeoxyglucose positron emission tomography (FDG-PET).<sup>4-7</sup> For example, in the case of FDG-PET imaging of breast cancer, tumor to nontumor signal ratios were significantly higher in 3 h than in 1.5 h images, and lesion detectability increased from 83% at 1.5 h to 93% at 3 h.<sup>7</sup> Similarly, dynamic FDG-PET scans were recorded with improved contrast between tumors and normal tissues at 2 h compared with 1 h postinjection of the tracer.<sup>8</sup> However, the application of this approach in the case of FDG-PET is limited by the short  $t_{1/2}$  of the <sup>18</sup>F tracer (109.7 min).<sup>9</sup> This limitation would not apply to an NIR-fluorescent probe.

Cyclooxygenase-2 (COX-2) is a promising target for molecular imaging because it is overexpressed in inflammation and many malignancies.<sup>10,11</sup> We recently discovered fluorocoxib A, a 5-carboxy-rhodamine-labeled COX-2 inhibitor, and described its utility in the selective visualization of COX-2 in inflammation and cancer.<sup>12</sup> The success of fluorocoxib A provides the proof-of-principle for COX-2-targeted imaging, but use of this agent has been limited to imaging within only a few hours following administration. Herein, we report the synthesis and evaluation of a long-lived COX-2-targeted NIR probe, fluorocoxib C (FC). FC is a potent and selective COX-2 inhibitor that exhibits COX-2-targeted uptake in human tumor xenografts in both prompt and delayed NIR imaging protocols. Furthermore, we show that delayed imaging using FC results in markedly improved contrast between signals in tumor and nontumor tissues.

Chemical synthesis of FC was accomplished using a conjugate chemistry strategy, in which treatment of indomethacin (Fig. 1) with mono *t*-butyloxycarbonyl (BOC) *n*-butyldiamine in the presence of ethyl-1-[3-(dimethylamino)propyl]-3-ethylcarbodiimide hydrochloride, a carboxyl activator, afforded *t*-butyl 4-[2-[1-(4-chlorobenzoyl)-5-methoxy-2-methyl-1*H*-indol-3-yl]acetamido]butylcarbamate. 1-Hydroxybenzotriazole hydrate was employed to prevent the generation of undesired *N*-acylurea by-products. Deprotection of the BOC group was cleanly and efficiently accomplished by bubbling hydrogen chloride gas through a solution of the compound in methylene chloride to afford *N*-(4-aminobutyl)-2-[1-(4-chlorobenzoyl)-5-methoxy-2-methyl-1*H*-indol-3-yl]acetamide hydrochloride.<sup>13</sup> Reaction of the succinimidyl ester of NIR664 with *N*-(4-aminobutyl)-2-[1-(4-chlorobenzoyl)-5-methoxy-2-methyl-1*H*-indol-3-yl]acetamide in dimethylsulfoxide using triethylamine as a base for 16 h at 25°C gave *N*-[(NIR664-yl)but-4-yl]-2-[1-(4-chlorobenzoyl)-5-methoxy-2-methyl-1*H*-indol-3-yl]acetamide (FC). [*Synthesis:* To a stirred solution of *N*-(4-aminobutyl)-2-[1-(4-chlorobenzoyl)-5-methoxy-2-methyl-1*H*-indol-3-yl]acetamide hydrochloride (0.05 mmol) in dimethylsulfoxide (5 ml), triethylamine (0.1 mmol) was added and stirred for 5 min at 25°C. Then *N*-succinimidyl ester of NIR664 (0.05 mmol) was added to the reaction mixture and stirred for 16 h at 25°C. The solvent was removed by lyophilization, and the crude product was purified by silica gel column chromatography CHCl<sub>3</sub>: MeOH:NH<sub>4</sub>OH (35:7:1) to give *N*-[(NIR664-yl)but-4-yl]-2-[1-(4-chlorobenzoyl)-5-methoxy-2-methyl-1*H*-indol-3-yl]acetamide as a green solid (68% yield), melting point 200 to 205°C (decompose), purity >99% by HPLC. <sup>1</sup>H NMR (400 MHz, DMSO-*d*<sub>6</sub>) δ 1.22 to 1.25 (m, 3H), 1.34 to 1.45 (m, 4H), 1.65 (s, 6H), 1.74 to 1.84 (m, 4H), 1.90 (s, 6H), 2.23

\*Address all correspondence to: Md. Jashim Uddin, E-mail: jashim.uddin@vanderbilt.edu

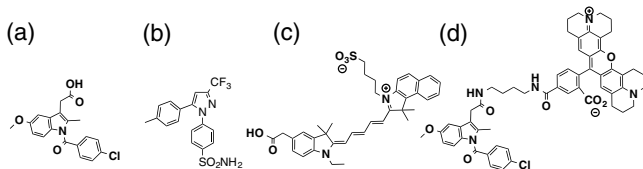


**Fig. 1** Structures of (a) indomethacin, (b) celecoxib (Cel), (c) NIR664 (NIR), and (d) fluorocoxib A (FA).

(s, 3H), 2.54 to 2.59 (m, 2H), 3.00 to 3.10 (m, 4H), 3.40 (s, 2H), 3.45 (s, 2H), 3.76 (s, 3H), 4.04 to 4.11 (m, 2H), 4.16 to 4.26 (m, 2H), 6.24 to 6.29 (m, 1H), 6.41 to 6.45 (m, 1H), 6.56 to 6.60 (m, 1H), 6.70 (dd,  $J = 9, 2.5$  Hz, 1H), 6.93 (d,  $J = 9$  Hz, 1H), 7.12 (d,  $J = 2.5$  Hz, 1H), 7.19 to 7.25 (m, 1H), 7.27 to 7.31 (m, 1H), 7.39 to 7.45 (m, 1H), 7.46 to 7.52 (m, 1H), 7.54 to 7.60 (m, 1H), 7.66 (d,  $J = 8.7$  Hz, 2H), 7.71 (d,  $J = 8.7$  Hz, 2H), 7.74 to 7.80 (m, 1H), 8.01 to 8.10 (m, 4H), 8.18 (d,  $J = 9.2$  Hz, 1H), 8.25 to 8.31 (m, 1H), 8.34 to 8.44 (m, 1H). Mass (ESI)  $m/z$  [M + H]<sup>+</sup> calcd 1036.44; found 1036.57.] The chemical structure of FC and its photophysical properties are described in Fig. 2.

The ability of FC to inhibit purified COX-1 or COX-2 was evaluated in a thin layer chromatography assay using <sup>14</sup>C-arachidonic acid.<sup>12</sup> FC displayed selective and potent COX-2 inhibitory activity (COX-2 IC<sub>50</sub> = 0.5 μM; COX-1 IC<sub>50</sub> > 25 μM) while NIR664 was inactive. Inhibition of COX-2 in intact cells by FC was also evaluated using a previously described method.<sup>12</sup> The IC<sub>50</sub> values for inhibition of COX-2 by FC in lipopolysaccharide (LPS)-activated RAW264.7 cells and human 1483 head and neck squamous cell carcinoma (HNSCC) cells were 0.37 and 0.32 μM, respectively.

We first evaluated the prompt optical imaging potential of FC to visualize COX-2 in a preclinical model of cancer. We implanted xenografts in female nude mice by subcutaneously injecting COX-2-expressing 1483 HNSCC cells in the left hip or COX-2-null human colorectal carcinoma (HCT116) cells in the right hip. The tumors were allowed to grow to approximately 700 to 1000 mm<sup>3</sup>. We administered FC or NIR664 at a low-dose (0.2 mg/kg, retro-orbitally) to the tumor-bearing animals. In some cases, the animals were pretreated with the COX-2-selective inhibitor celecoxib (2 mg/kg) prior to FC injection. The animals were imaged at 4 h postinjection of fluorophore on a Xenogen IVIS 200 optical imaging system. The imaging showed good uptake of FC into the COX-2-expressing 1483 HNSCC tumors while minimal uptake was documented in the COX-2-negative HCT116 tumors or in 1483 HNSCC tumors pretreated with celecoxib or imaged using NIR664 dye instead

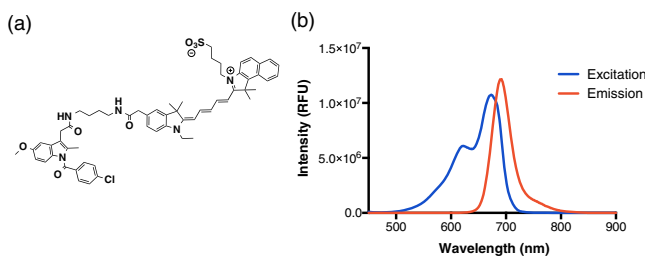


**Fig. 2** (a) Structure of fluorocoxib C (FC). (b) Steady state fluorescence excitation and emission spectra were determined for FC in water pH 7 using a Spex 1681 Fluorolog spectrofluorometer, equipped with a 450 W xenon arc lamp. The excitation and emission monochromator slit widths were 1 to 2 nm. FC exhibited excitation and emission maxima of  $\lambda_{ex} = 672$  nm and  $\lambda_{em} = 692$  nm, respectively.

of FC [Figs. 3(a)–3(d)]. To confirm COX-2-dependent uptake of FC, we collected the tumors by dissection and imaged them *ex vivo* under the Xenogen IVIS 200 optical imaging system. Figures 3(e)–3(h) show the tumor images with uptake quantification provided in Fig. 3(i). After imaging, we analyzed the tumor tissues using LC-MS/MS and identified the intact parent FC in the 1483 HNSCC tumors (0.24 pmol/g tissue,  $n = 3$ ).

These prompt imaging experiments established that FC is a valid COX-2-targeting NIR probe. However, at this 4-h time point, substantial fluorescent signals are also detectable in the peritoneal cavity due to biodistribution of the probe in abdominal organs. This led us to investigate whether these nonspecific signals would clear with time such that only the fluorescence signal would be detectable in the tumor. A group of female nude mice bearing 1483 HNSCC xenograft tumors (750 to 1000 mm<sup>3</sup>) on their left hip was dosed by injection with a low dose of FC (0.2 mg/kg). The animals were lightly anesthetized with 2% isoflurane and imaged on a Xenogen IVIS 200 optical imaging system at varying times up to 7 days after FC administration. Control animals that did not receive an FC injection showed a noticeable autofluorescence in both sides of the peritoneal cavity but no signal at the tumor [Fig. 4(a)]. In FC-injected animals, the fluorescence signal was reproducibly detected in the tumor at 3 h and

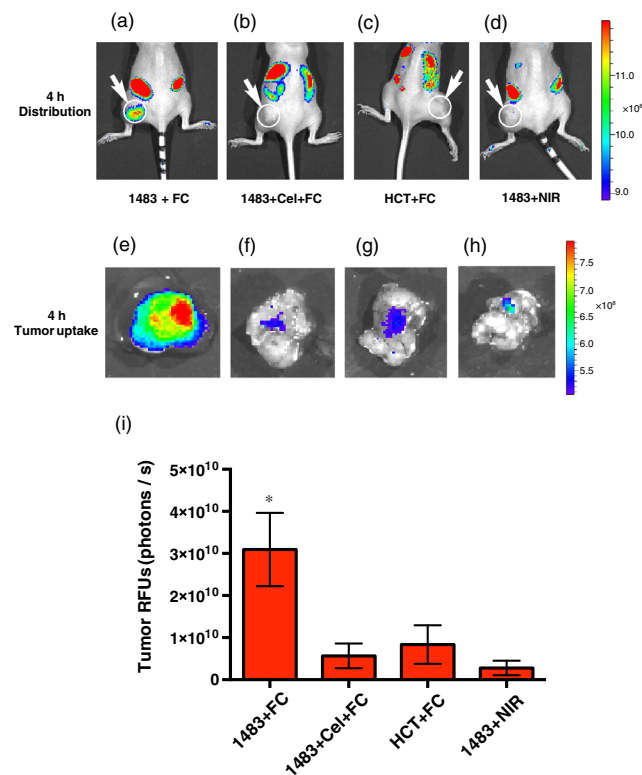


**Fig. 3** *In vivo* and *ex vivo* prompt imaging of COX-2 in 1483 HNSCC xenograft tumors. FC (0.2 mg/kg, r.o.) or NIR664 (0.2 mg/kg, r.o.) were injected into nude mice bearing 1483 HNSCC or HCT116 xenograft tumors and imaged at 4 h postinjection under a Xenogen IVIS 200 optical imaging system. *In vivo* image of (a) 1483 HNSCC xenograft with FC; (b) celecoxib pretreated 1483 HNSCC xenograft with FC; (c) HCT116 xenograft with FC; and (d) 1483 HNSCC xenograft with NIR664. After imaging, tumors were collected by dissection and imaged under a Xenogen IVIS 200 optical imaging system. *Ex vivo* image of (e) 1483 HNSCC tumor shown in (a); (f) 1483 HNSCC tumor shown in (b); (g) HCT116 tumor shown in (c); and (h) 1483 HNSCC tumor shown in (d). (i) Quantification of tumor uptake of FC by *ex vivo* image analysis using AMIDE software ( $n = 4, p < 0.003$ ).

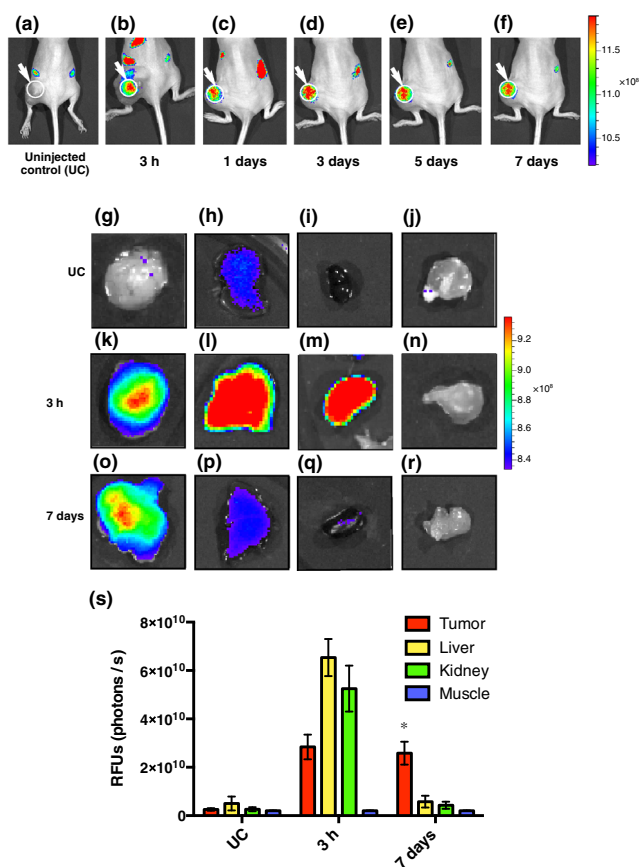


**Fig. 4** *In vivo* and *ex vivo* delayed optical imaging of COX-2 in 1483 HNSCC xenograft tumors. FC was injected into nude mice bearing 1483 HNSCC xenograft tumor on the left hip (0.2 mg/kg, r.o.). The animal was imaged from 3 h to 7 days postinjection of FC under a Xenogen IVIS 200 optical imaging system: (a)–(f) Fluorescence images of a nude mice bearing 1483 HNSCC xenograft at 3 h to 7 days postinjection of FC. (g)–(j) Fluorescence images of tumor, liver, kidney, and muscle from an uninjected animal. (k)–(n) Fluorescence images of tumor, liver, kidney, and muscle from a 3 h animal. (o)–(r) Fluorescence images of tumor, liver, kidney, and muscle from a 7-days animal. (s) Quantification of signals in tumor, liver, kidney, and muscle from uninjected control, 3 h and 7-days animals by AMIDE software ( $n = 4$ ,  $p = 0.004$ ).

persisted through the delayed imaging periods at 1, 3, 5, and 7 days postinjection. The delayed imaging showed a gradual decrease of peritoneal signals, resulting in a high signal-to-noise ratio at 7 days postinjection [Figs. 4(b)–4(f)]. After imaging, we euthanized the animals and collected tumor, liver, kidney, and muscle from uninjected control animals and from FC-injected animals at 3 h and 7 days following FC administration. *Ex vivo* imaging under a Xenogen IVIS 200 optical imaging system of uninjected organs showed minimal autofluorescence in the tumor, kidney, or muscle, with a fair amount of signal in liver [Figs. 4(g)–4(j)]. The 3 h FC-treated organs showed a significant uptake in the tumor, liver, and kidney, with minimal uptake in the muscle [Figs. 4(k)–4(n)]. The 7 days FC-treated organs showed low signals in the liver, kidney, and muscle that were comparable with the liver, kidney, and muscle signals from uninjected animals, but the tumor signal remained comparable with the

tumor signal at the 3 h time point [Figs. 4(o)–4(r)]. Figure 4(s) presents the quantification of signals in tumor, liver, kidney, and muscle from uninjected controls, and from 3 h and 7 days FC-treated animals by AMIDE software. Dynamic changes in signals in the nonspecific organs are due to the clearance from the normal tissues.

In conclusion, we report the discovery of FC, a COX-2-targeted NIR probe. Uptake of FC is COX-2-dependent as demonstrated by the lack of uptake of nontargeted NIR664 and by the failure of FC uptake in celecoxib-pretreated or COX-2-negative tumors. In addition, FC is effective as a delayed fluorescence imaging agent exhibiting the potential for improved lesion detection accuracy over standard imaging through improved signal-to-noise in differentiating tumor from nontumor tissues. Thus, FC represents the first delayed COX-2-targeted fluorescence imaging NIR probe for detection of tissues containing elevated levels of COX-2 in preclinical and clinical settings.

### Acknowledgments

This work was supported by research grants from the National Institutes of Health numbers CA128323-4,-5 (MJU), CA182850-01A1 (MJU), CA136465 (LJM), and CA89450 (LJM). We are grateful to the Small Molecule NMR Core and the Mass Spectroscopy Research Center for compound characterizations.

### References

1. R. Weissleder et al., "In vivo imaging of tumors with protease-activated near-infrared fluorescent probes," *Nat. Biotechnol.* **17**, 375–378 (1999).
2. S. B. Mondol et al., "Real-time fluorescence image-guided oncologic surgery," *Adv. Cancer Res.* **124**, 171–211 (2014).
3. C.-H. Tung et al., "A receptor-targeted near-infrared fluorescence probe for in vivo tumor imaging," *ChemBioChem* **3**, 784–786 (2002).
4. R. Kubota et al., "Microautoradiographic study for the differentiation of intratumoral macrophages, granulation tissues and cancer cells by the dynamics of fluorine-18-fluorodeoxyglucose uptake," *J. Nucl. Med.* **35**(1), 104–112 (1994).
5. V. J. Lowe et al., "Optimum scanning protocol for FDG-PET evaluation of pulmonary malignancy," *J. Nucl. Med.* **36**(5), 883–887 (1995).
6. L. M. Hamberg et al., "The dose uptake ratio as index of glucose metabolism: useful parameter or oversimplification?" *J. Nucl. Med.* **35**(8), 1308–1312 (1994).
7. A. R. Boemer et al., "Optimal scan time for fluorine-18 fluorodeoxyglucose positron emission tomography in breast cancer," *Eur. J. Nucl. Med.* **26**, 226–230 (1999).
8. K. Hamada et al., "Evaluation of delayed <sup>18</sup>F-FDG PET in differential diagnosis for malignant soft-tissue tumors," *Ann. Nucl. Med.* **20**(10), 671–675 (2006).
9. C.-Y. Shiu et al., "Synthesis and specific activity determination of NCA <sup>18</sup>F-labeled butyrophenone, neuroleptics: benperidol, haloperidol, spiperidol and pipamperone," *J. Nucl. Med.* **26**(2), 181–186 (1985).
10. C. S. Williams et al., "The role of cyclooxygenases in inflammation, cancer, and development," *Oncogene* **18**(55), 7908–7916 (1999).
11. V. N. Shirvani et al., "Cyclooxygenase 2 expression in Barrett's esophagus and adenocarcinoma: ex vivo induction by bile salts and acid exposure," *Gastroenterology* **118**, 487–496 (2000).
12. M. J. Uddin et al., "Selective visualization of cyclooxygenase-2 in inflammation and cancer by targeted fluorescent imaging agents," *Cancer Res.* **70**, 3618–3627 (2010).
13. M. J. Uddin et al., "Design, synthesis, and structure: activity relationship studies of fluorescent inhibitors of cyclooxygenase-2 as targeted optical imaging agents," *Bioconjugate Chem.* **24**, 712–723 (2013).